

Leptonic anomalous gauge couplings detection on electron positron colliders

Sheng-Zhi Zhao, Bin Zhang*

*Department of Physics, Tsinghua University, Beijing, 100084, China and
Center for High Energy Physics, Tsinghua University, Beijing, 100084, China*

We studied the dimension-6 leptonic anomalous gauge couplings in the formulation of linearly realized gauge symmetry effective Lagrangian and investigated the constrain on these anomalous couplings from the existed experiments data including LEP2 and W boson decay. Some very loose bounds of $O(1 - 10)\text{TeV}^{-2}$ on four relevant anomalous couplings are given by LEP2. We research the sensitivity of testing the leptonic anomalous couplings via the process $e^+e^- \rightarrow W^+W^-$ at future e^+e^- linear colliders. We discussed different sensitive anomalous couplings at polarized and unpolarized e^+e^- colliders, respectively, with 500GeV and 1TeV collision energy. Our results show that the a 500GeV ILC can provide a test of the anomalous couplings, with the same relative uncertainty of cross section measurement, of $O(10^{-3} - 10^{-2})\text{TeV}^{-2}$, and a 1 TeV ILC can test the anomalous couplings of $O(10^{-4} - 10^{-3})\text{TeV}^{-2}$.

PACS numbers: 12.60.Cn, 13.66.Jn, 14.60.Cd, 14.70.-e

INTRODUCTION

The effective Lagrangian always has been an important model independent approach to study the new physics beyond standard model(SM). It is customary to formulate new physics effects by linearly realizing the gauge symmetry [1, 2]. After integrating out heavy degrees of freedom at the scale, the leading effects at low energies can be parameterized by the effective interactions. Literature[1] had systemically given all the the gauge-invariant dimension-6 operators which can be constructed from the standard model fields. The coefficients of these anomalous operators, which are called "anomalous couplings", reflect the strength of the new physics effects at low energies. There are already many theoretical studies which have been suggested to test the anomalous gauge couplings of the Higgs boson and gauge

bosons in the literature for the LHC [3–7], and for the ILC [8–10]. However, there has not been much work on how to detect the anomalous gauge couplings of the fermions at colliders.

Since the discovery of neutrino oscillations in recent years[11], the flavor physics about leptons, in particular, the neutrino mass and flavor mixing become a hot topic in particle physics. Many theoretical models introduced the heavy neutrinos or the fourth generation leptons to explain the small neutrino masses[12]. In these models, the small neutrino masses were given by the seesaw mechanism. The seesaw mechanism generally requires heavy neutrino mass or very massive fourth generation lepton. It is very difficult to detect these particles directly at LHC or other future colliders. However, the effects of those extra massive particles can be reflected on the anomalous couplings of leptons and gauge bosons in the low-energy effective Lagrangian. The measurement of the phenomenological effects of these leptonic anomalous gauge couplings on colliders will be useful in understanding the new physics beyond the standard model about the lepton and neutrino. Furthermore, many new physical models about the electroweak spontaneous symmetry breaking, such as little Higgs models[13], Higgsless models[14] and Left-Right symmetric gauge models[15], introduced some extra gauge bosons which mixing with ordinary gauge bosons. There will be anomalous couplings different from standard model between the fermions and the ordinary gauge bosons in those models. Detecting these leptonic anomalous gauge couplings on colliders also can test and verify those electroweak new physical models.

In this paper, we proposed the process $e^+e^- \rightarrow W^+W^-$ at the future electron-positron linear collider (ILC) to detect the anomalous couplings between the electron and the W , Z gauge bosons. This process is the simplest process at e^+e^- colliders, and both W and Z gauge couplings involve in the process $e^+e^- \rightarrow W^+W^-$.

In the standard model $e^+e^- \rightarrow W^+W^-$ process, the E^2 terms in the amplitude cancel each other between different Feynman diagrams, and the total amplitude and cross section do not increase with collision energy. If anomalous couplings exist, the cancelation of energy power will be destroyed. Furthermore, the anomalous couplings will result in higher energy power dependence. Therefore, the existing low energy electron-positron experiments give a very weak limit on the anomalous couplings, while the anomalous couplings are more likely to be detected on the future high-energy colliders.

THE LEPTONIC ANOMALOUS GAUGE COUPLINGS IN EFFECTIVE LAGRANGIAN

To extend the structure of the SM in a model-independent approach, it is customary to formulate new physics effects by linearly realizing the gauge symmetry. After integrating out heavy degrees of freedom at the high scale Λ , the leading effects at low energies can be parameterized by the effective interactions

$$\mathcal{L}_{\text{eff}} = \sum_n \frac{f_n}{\Lambda^2} \mathcal{O}_n, \quad (1)$$

where f_n 's are dimensionless anomalous couplings, and \mathcal{O}_n 's the gauge-invariant dimension-6 operators, constructed from the SM fields. C. N. Leung, S. T. Love and S. Rao [1] described all the dimension-6 $SU_c(3) \times SU_W(2) \times U(1)$ gauge invariant operators. While, in all these operators, there are six operators of them are involved with leptonic gauge couplings and CP even, they are:

$$\begin{aligned} \mathcal{O}_7^{VF} &= i\bar{L}\gamma_\mu W^{\mu\nu} \overleftrightarrow{D}_\nu L, \\ \mathcal{O}_{11}^{VF} &= i\bar{L}\gamma_\mu B^{\mu\nu} \overleftrightarrow{D}_\nu L, \\ \mathcal{O}_{13}^{VF} &= i\bar{E}\gamma_\mu B^{\mu\nu} \overleftrightarrow{D}_\nu E, \\ \mathcal{O}_{24}^{VF} &= \bar{L}\gamma_\mu (D_\nu W^{\mu\nu}) L, \\ \mathcal{O}_{26}^{VF} &= \bar{L}\gamma_\mu \partial_\nu B^{\mu\nu} L, \\ \mathcal{O}_{27}^{VF} &= \bar{E}\gamma_\mu \partial_\nu B^{\mu\nu} E. \end{aligned}$$

here, L is left-hand $SU_W(2)$ lepton doublet and E is lepton right-hand singlet.

The Feynman rules of the vertices with leptons and gauge bosons are listed in appendix. From these vertices, we can find that the operator \mathcal{O}_7 and \mathcal{O}_{24} can affect all the vertices between leptons and gauge bosons in the process $e^+e^- \rightarrow W^+W^-$. These two operators even provide a additional 4-line $l^+l^-W^+W^-$ vertex. However, other operators \mathcal{O}_{11} , \mathcal{O}_{13} , \mathcal{O}_{26} and \mathcal{O}_{27} only affect the neutral current vertices. Therefore, the process $e^+e^- \rightarrow W^+W^-$ is much more sensitive to operators \mathcal{O}_7 and \mathcal{O}_{24} than others. The two operators \mathcal{O}_{11} and \mathcal{O}_{13} are only involved in the initial electron positron fusion vertices in the S channel diagrams, and the three momentums of the neutral current vertices are parallel. The construction

of the two operators' Feynman rules determine their contribution are zero when all three momentums are parallel as we can see from the Feynman rule (b) in the Appendix.

THE CONSTRAINS FROM LEP2 AND W DECAY

The measurement on the total cross section of W pair production on experiment LEP2[16] can give some limits on the anomalous coupling constants. However, because the collision energy is just beyond the W pair threshold, the W bosons product at LEP2 do not have much high momentum. The effect of dimension-6 operators are very small, in other words, the constraints from LEP2 are very weak.

In this work, we only calculate the cross section of $e^+e^- \rightarrow W^+W^-$ at tree level, and figure out the relative deviations from standard model caused by various anomalous couplings. We assume reasonably that the relative deviation will not be changed a lot by radiative correction and detector simulation. The LEP2 experimental measurement on the cross section of the process $e^+e^- \rightarrow W^+W^-$ is highly consistent with theoretical calculation. The systematic uncertainty of experimental measurement can conversely give the constrains on the anomalous couplings. The relative uncertainty of cross section measurement is about $\pm 2\%$ at LEP2[16]. Here, we conservatively enlarged the experimental uncertainty and theoretical uncertainty to $\pm 5\%$, any cross section deviations beyond $\pm 5\%$ caused by anomalous couplings can be detected at colliders. We also suppose the same uncertainty for future linear colliders.

In order to accord the experiment, we let the final W bosons decay to fermions and imposed the following acceptance cuts on final fermions:

$$|\eta| < 3, \quad p_T > 10\text{GeV}.$$

After the cuts, the standard model detectable W pair product cross section is 17.7pb at tree level. Fig.1 plots the relative deviations caused respectively by different anomalous coupling constants.

According the experimental relative uncertainty $\pm 5\%$, the LEP2 measurement on the cross section can provide the limits on anomalous couplings:

$$\begin{aligned} -2.7 \text{ TeV}^{-2} &< f_7/\Lambda^2 < 2.7 \text{ TeV}^{-2}, \\ -9.8 \text{ TeV}^{-2} &< f_{24}/\Lambda^2 < 1.8 \text{ TeV}^{-2}, \end{aligned}$$

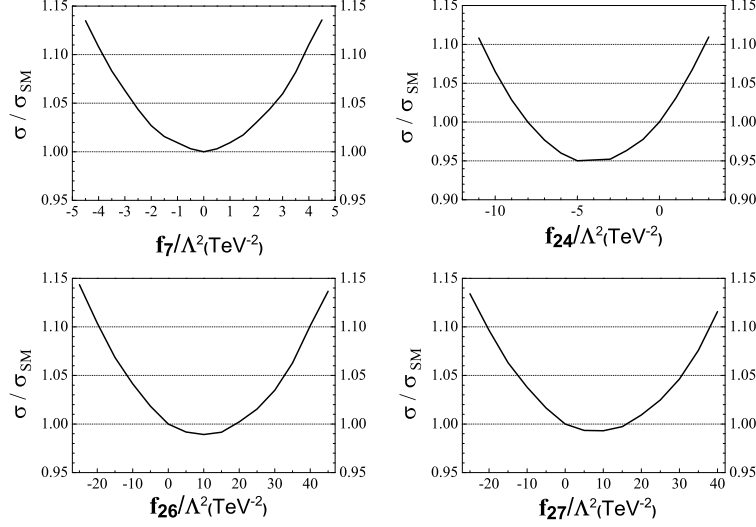


FIG. 1: The relative deviations of $e^+e^- \rightarrow W^+W^-$ cross section on LEP2 caused by different anomalous coupling constants.

$$\begin{aligned} -11 \text{ TeV}^{-2} &< f_{26}/\Lambda^2 < 33 \text{ TeV}^{-2}, \\ -13 \text{ TeV}^{-2} &< f_{27}/\Lambda^2 < 30 \text{ TeV}^{-2}. \end{aligned}$$

The bounds on the four relevant anomalous couplings from LEP2 experiment are very loose, because the outgoing W bosons do not obtain large momentums compared to their mass. However, the dimension-6 anomalous couplings should be enhanced by large momentums.

The W boson decay width and the leptonic branching ratio with very high measurement accuracy also can provide the limits on anomalous couplings, however only one anomalous coupling f_{24} can will change the W decay amplitude. The Fig.2 plotted the relative deviations on W boson leptonic decay partial width caused by the anomalous coupling constants f_{24} . The f_{24} anomalous coupling can increase or decrease the leptonic decay partial width, because of the interference with the standard vertex.

The experimental relative uncertainty on W boson decay width and the leptonic branching ratio are very small, both within $\pm 2\%$ [17], so the relative uncertainty of the leptonic decay partial width is also within $\pm 2\%$. Therefore, the measurement on W boson decay can provide a more stringent limit on anomalous coupling f_{24} :

$$-1.1 \text{ TeV}^{-2} < f_{24}/\Lambda^2 < 1.1 \text{ TeV}^{-2},$$

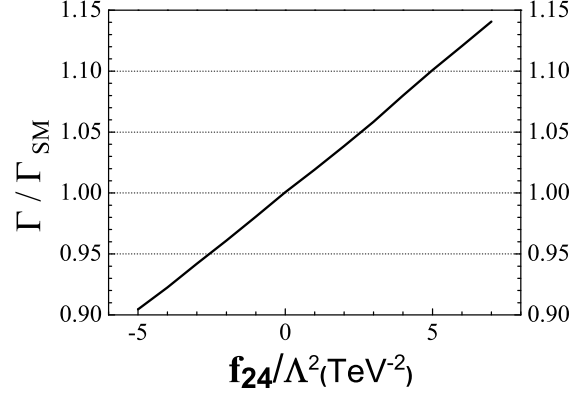


FIG. 2: The relative deviations of W boson leptonic decay partial width caused by the anomalous coupling constants f_{24} .

THE DETECTION OF LEPTONIC ANOMALOUS GAUGE COUPLINGS ON ILC

The anomalous couplings bring high energy power dependence to the $e^+e^- \rightarrow W^+W^-$ cross section. The higher the collision energy, the greater the deviation caused by anomalous couplings. We considered the relative deviations caused by different anomalous couplings on future ILC with the collision energy $\sqrt{s_{ee}} = 500$ GeV in Fig.3, and on $\sqrt{s_{ee}} = 1$ TeV ILC in Fig.4. The total cross section decreases as the collision energy increases and concentrated in the forward region, and the quarks or leptons decay from the energetic W bosons are following the forward alignment, so the basic acceptance cuts reduce the cross section more severely. The standard model total cross section after basic cuts is about 5.68pb as $\sqrt{s_{ee}} = 500$ GeV and 1.42pb as $\sqrt{s_{ee}} = 1$ TeV. However, the larger luminosity of ILC will still provide sufficient events to analysis the effect of the anomalous couplings. We also suppose the ILC can reach the same experimental relative uncertainty on cross section as LEP2 and the constraint on the detect ability still come from the experimental uncertainty.

The detection ability of high energy ILC is much more sensitive than LEP2. If we also suppose the same experimental relative uncertainty of cross section on ILC as $\pm 5\%$, the detection sensitivity on the anomalous coupling constants of $\sqrt{s_{ee}} = 500$ GeV ILC are:

$$\begin{aligned}
 -0.18 \text{ TeV}^{-2} &< f_7/\Lambda^2 < 0.18 \text{ TeV}^{-2}, \\
 -0.042 \text{ TeV}^{-2} &< f_{24}/\Lambda^2 < 0.14 \text{ TeV}^{-2}, \\
 -2.3 \text{ TeV}^{-2} &< f_{26}/\Lambda^2 < 8.6 \text{ TeV}^{-2},
 \end{aligned}$$

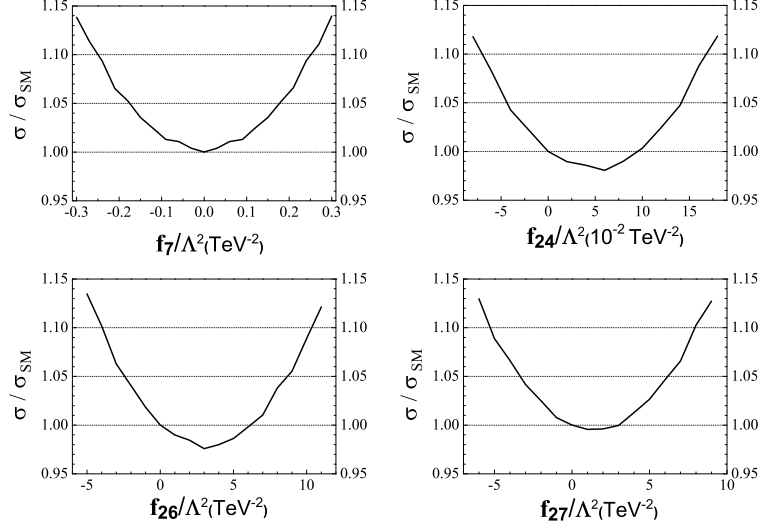


FIG. 3: The relative deviations of $e^+e^- \rightarrow W^+W^-$ cross section on 500GeV ILC caused by various anomalous couplings.

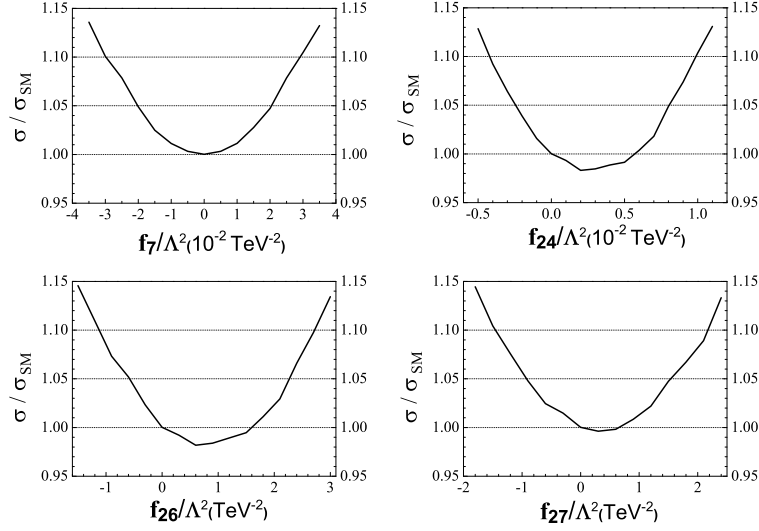


FIG. 4: The relative deviations of $e^+e^- \rightarrow W^+W^-$ cross section on 1TeV ILC caused by various anomalous couplings.

$$-3.3 \text{ TeV}^{-2} < f_{27}/\Lambda^2 < 6.2 \text{ TeV}^{-2}.$$

And, the detection sensitivities on the anomalous coupling constants of $\sqrt{s_{ee}} = 1000 \text{ GeV}$ ILC are:

$$-2.0 \times 10^{-2} \text{ TeV}^{-2} < f_7/\Lambda^2 < 2.0 \times 10^{-2} \text{ TeV}^{-2},$$

$$\begin{aligned}
-2.5 \times 10^{-3} \text{ TeV}^{-2} &< f_{24}/\Lambda^2 < 8.0 \times 10^{-3} \text{ TeV}^{-2}, \\
-0.6 \text{ TeV}^{-2} &< f_{26}/\Lambda^2 < 2.3 \text{ TeV}^{-2}, \\
-0.9 \text{ TeV}^{-2} &< f_{27}/\Lambda^2 < 1.5 \text{ TeV}^{-2}.
\end{aligned}$$

The detection sensitivities are increased by 1-2 orders of magnitude than the LEP2.

THE W BOSONS' ANGULAR DISTRIBUTION OF THE ANOMALOUS SIGNATURE

We also analyzed the distribution of cross section in order to find the sensitive region of the anomalous coupling. The W outgoing angular is the unique kinematic parameter in the process $e^+e^- \rightarrow W^+W^-$ at the energy determined e^+e^- colliders, and the W angular can be reconstructed by the W decay final states on ILC. Therefore, we analyzed the angular distribution of the final state W particle, and compared the distribution differences between anomalous couplings and the standard model.

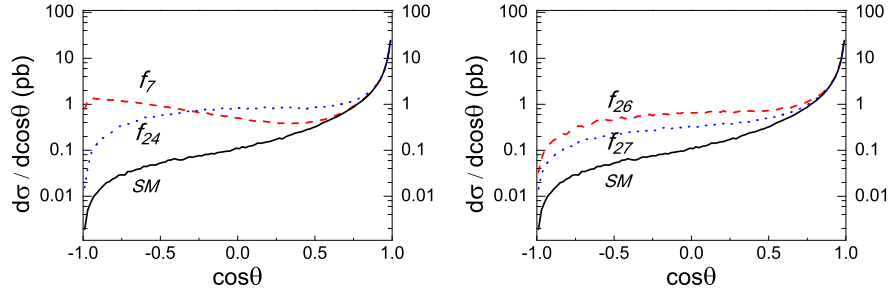


FIG. 5: The W boson outgoing angular distribution at 1TeV ILC. The solid curve is the SM distribution, the dashed and dotted curves are the distributions respectively with $f_7/\Lambda^2 = 8 \times 10^{-2} \text{ TeV}^{-2}$; $f_{24}/\Lambda^2 = 2 \times 10^{-2} \text{ TeV}^{-2}$; $f_{26}/\Lambda^2 = 6 \text{ TeV}^{-2}$; $f_{27}/\Lambda^2 = 3 \text{ TeV}^{-2}$.

Fig.5 and 6 show the differences on W^- boson outgoing angular distribution, where θ_{W^-} is the W^- production angle with respect to the direction of the incoming electrons. The distribution of the W^+ production angle with respect to the direction of the incoming positrons θ_{W^+} is same for the charge symmetry. In order to give the distribution of the angle of the W^- or W^+ bosons, it is necessary to distinguish the sign of the W charge in the experiment. Therefore, Only the semileptonic decay of the W pairs can be considered, $e^+e^- \rightarrow W^+W^- \rightarrow qq\ell\nu$, here the final leptons only include μ^\pm and e^\pm . So the semileptonic

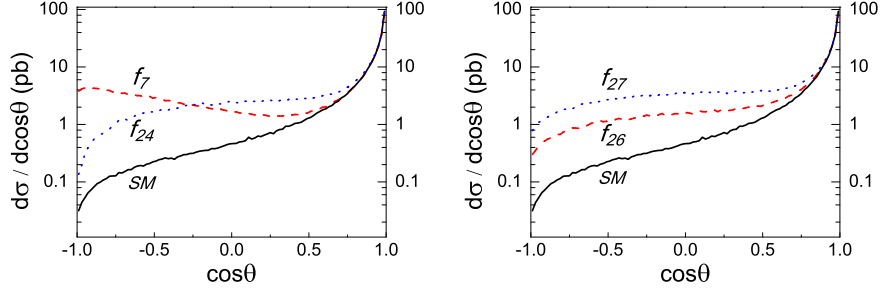


FIG. 6: The W boson outgoing angular distribution at 500 GeV ILC. The solid curve is the SM distribution, the dashed and dotted curves are the distributions respectively with $f_7/\Lambda^2 = 0.6 \text{ TeV}^{-2}$; $f_{24}/\Lambda^2 = 0.3 \text{ TeV}^{-2}$; $f_{26}/\Lambda^2 = 15 \text{ TeV}^{-2}$; $f_{27}/\Lambda^2 = 20 \text{ TeV}^{-2}$.

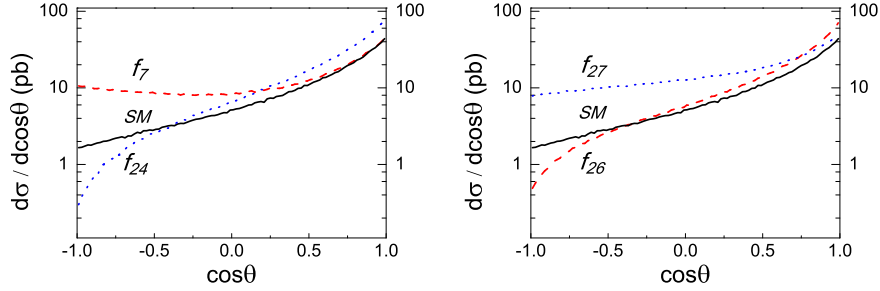


FIG. 7: The W boson outgoing angular distribution at 200 GeV LEP2. The solid curve is the SM distribution, the dashed and dotted curves are the distributions respectively with $f_7/\Lambda^2 = 8 \text{ TeV}^{-2}$; $f_{24}/\Lambda^2 = 9 \text{ TeV}^{-2}$; $f_{26}/\Lambda^2 = 60 \text{ TeV}^{-2}$; $f_{27}/\Lambda^2 = 90 \text{ TeV}^{-2}$.

decay branching ratio is $66\% \times 21\% \times 2 = 27.7\%$. For the standard model, the cross section is mainly distributed in the forward region where $\cos \theta_{W\pm}$ close to one, because the T channel neutrino exchange diagram is dominant. The anomalous couplings' relative effect to the cross section is much larger in the small $\cos \theta_{W\pm}$ area, but the partial cross section in this region is very small as show in the figures. The trend becomes more obvious with the higher the collision energy. The standard model cross section within $\cos \theta_{W\pm} < 0.75$ is 0.28 pb on 1 TeV ILC, and decreases to $0.146(0.053) \text{ pb}$ within $\cos \theta < 0.5(0)$. If the integrated luminosity of ILC is large enough (for example, $\int \mathcal{L} \geq 46.2 \text{ fb}^{-1}$), one can apply a W angular cut (for instance $\cos \theta < 0.75$) to improve the detection sensitivity. In this case, the standard model will provide more than $\sigma_{SM}(\cos \theta < 0.75) \times Br \times \int \mathcal{L} = 3600$ events, and the significance of 5% relative deviation caused by anomalous couplings will be greater than 3σ (the significance

defined as $N_s/\sqrt{N_B}$). If the integrated luminosity becomes greater, we can take a more stringent W angular cut. The cut $\cos\theta < 0.5$ can be applied and still keep 3σ significance when $\int \mathcal{L} \geq 90.2\text{fb}^{-1}$ and the cut $\cos\theta < 0$ can be applied if $\int \mathcal{L} \geq 245\text{fb}^{-1}$ as listed in Table I. The total cross section at 500GeV ILC is larger than 1TeV ILC, and the effect of W outgoing angular cut at 500GeV ILC is not as obvious as at 1TeV ILC, so the requirement of the integrated luminosity is much smaller. For the process on 200GeV LEP2, as shown in Fig.7, the outgoing W bosons are not very forward because the W momentum is small compared to its rest mass. The W outgoing angular cut at the 200GeV LEP2 is almost not helpful to improve the detection limits of anomalous couplings, expect a little improvement on f_7 .

TABLE I: The cross sections after different W angular cuts on $\sqrt{s_{ee}} = 500$ GeV and 1TeV ILC and the required integrated luminosity for 5% relative deviation to keep 3σ significance.

$\cos\theta$ cut	σ (500 GeV)	required $\int \mathcal{L}$	σ (1 TeV)	required $\int \mathcal{L}$
none	5.68 pb	0.63 fb^{-1}	1.42 pb	2.5 fb^{-1}
$\cos\theta < 0.75$	1.14 pb $\times 27.7\%$	11.2 fb^{-1}	0.28 pb $\times 27.7\%$	46.2 fb^{-1}
$\cos\theta < 0.5$	0.61 pb $\times 27.7\%$	21.3 fb^{-1}	0.146 pb $\times 27.7\%$	90.2 fb^{-1}
$\cos\theta < 0$	0.23 pb $\times 27.7\%$	56.3 fb^{-1}	0.053 pb $\times 27.7\%$	245 fb^{-1}

The more stringent W angular cut can give the better sensitivity on anomalous couplings detection, meanwhile the remained cross section is less and the more integrated luminosity is needed as listed in Table.I. The relative deviations caused by various anomalous couplings after the W outgoing angular cut $\cos\theta < 0$ are shown in Fig.8 as an example, where the collision energy $\sqrt{s_{ee}} = 1$ TeV.

From Fig.8, we can see that some specific anomalous coupling values can reduce the final cross section beyond 5%. The cross section decreases because of the interference between the anomalous couplings and the standard model couplings.

Table II and Table III give the detection limits of the $\sqrt{s_{ee}} = 500$ GeV and 1 TeV ILC respectively. Within the limits, the relative deviations on the cross section caused by anomalous couplings are less than $\pm 5\%$ which can not be detected at ILC. If any listed anomalous couplings beyond the bounds, the ILC can figure out the difference from the standard model. The more stringent W angular cut is applied, the better detection sensitivity ILC can pro-

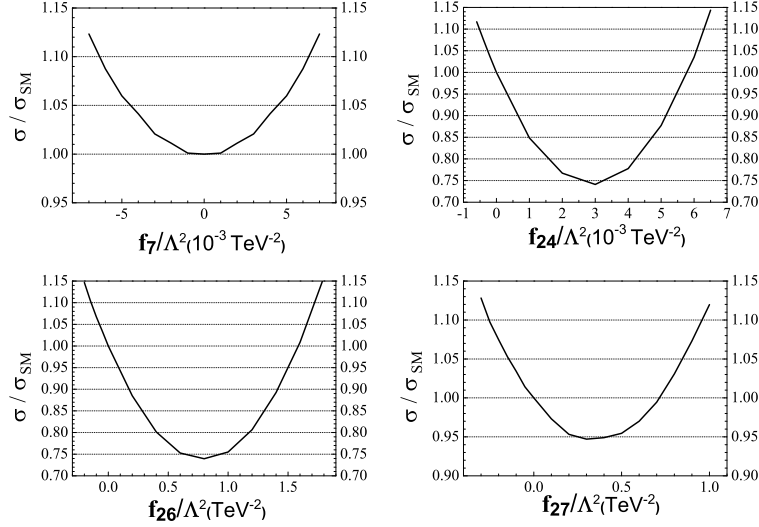


FIG. 8: The relative deviations of $e^+e^- \rightarrow W^+W^-$ cross section on 500GeV ILC caused by different anomalous coupling constants.

TABLE II: The detection limits of the anomalous coupling constants on $\sqrt{s_{ee}} = 500$ GeV ILC with different W outgoing angular cuts.

$\cos \theta$ cut	$f_7/\Lambda^2(10^{-2}\text{TeV}^{-2})$	$f_{24}/\Lambda^2(10^{-2}\text{TeV}^{-2})$	$f_{26}/\Lambda^2(10^{-1}\text{TeV}^{-2})$	$f_{27}/\Lambda^2(\text{TeV}^{-2})$
none	$-18 \sim 18$	$-4.2 \sim 14$	$-23 \sim 86$	$-3.3 \sim 6.2$
$\cos \theta < 0.75$	$-8 \sim 8$	$-1.1 \sim 1.5$	$-6.4 \sim 8.1$	$-1.2 \sim 4.0$
$\cos \theta < 0.5$	$-5.9 \sim 5.9$	$-0.67 \sim 0.95$	$-4.1 \sim 4.9$	$-0.76 \sim 3.6$
$\cos \theta < 0$	$-3.8 \sim 3.8$	$-0.44 \sim 0.5$	$-2.5 \sim 2.8$	$-0.49 \sim 0.99$

vide. We can see from Table III, after W angular cut, the ILC detection sensitivity are increased by 3-4 orders of magnitude than the LEP2.

THE POLARIZATION SCHEME

We also considered ILC with the polarization scheme. Both in standard model and anomalous couplings, the W boson only has coupling to left handed leptons. If the initial electrons are right handed polarized, they only couple to neutral gauge boson Z and γ . So the process $e_L^+e_R^- \rightarrow W^+W^-$ only has Z/γ S channel Feynman diagrams. Therefore the ILC with polarization scheme will be very useful to detect the anomalous coupling between lepton and Z boson. The standard model's right handed polarized cross section is 107fb

TABLE III: The detection limits of the anomalous coupling constants on $\sqrt{s_{ee}} = 1$ TeV ILC with different W outgoing angular cuts.

$\cos \theta$ cut	$f_7/\Lambda^2(10^{-3}\text{TeV}^{-2})$	$f_{24}/\Lambda^2(10^{-4}\text{TeV}^{-2})$	$f_{26}/\Lambda^2(10^{-1}\text{TeV}^{-2})$	$f_{27}/\Lambda^2(10^{-1}\text{TeV}^{-2})$
none	$-20 \sim 20$	$-25 \sim 80$	$-6 \sim 23$	$-9 \sim 15$
$\cos \theta < 0.75$	$-9.5 \sim 9.5$	$-6.7 \sim 10$	$-1.9 \sim 2.3$	$-3.3 \sim 10$
$\cos \theta < 0.5$	$-6.5 \sim 6.5$	$-4.2 \sim 5.0$	$-1.1 \sim 1.4$	$-2.0 \sim 9.2$
$\cos \theta < 0$	$-4.6 \sim 4.6$	$-2.8 \sim 2.9$	$-0.75 \sim 0.78$	$-1.4 \sim 2.5$

with $\sqrt{s_{ee}} = 500$ GeV and 22.2fb with $\sqrt{s_{ee}} = 1$ TeV. The cross section is still large enough to analysis $\pm 5\%$ relative deviation with a certain integrated luminosity.

It is different from unpolarized ILC scheme, the process with right handed polarized electrons is very sensitive to the coefficient f_{27} which only appears in the anomalous coupling between lepton and Z boson and not sensitive on unpolarized $e^+e^- \rightarrow W^+W^-$ process. In polarized S channel process, the anomalous coupling f_{27} can interfere with standard coupling, and the relative deviations on cross section are shown in Fig.9.

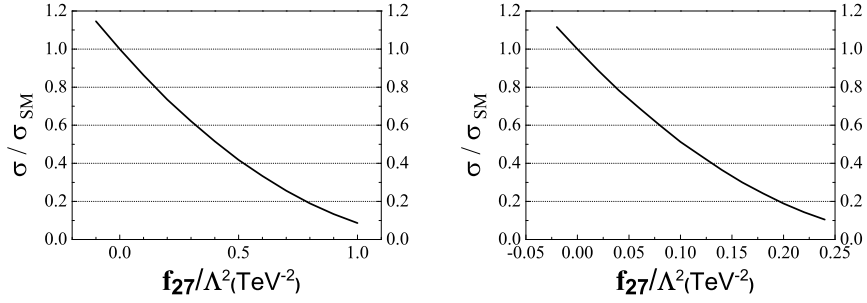


FIG. 9: The relative deviations of $e_L^+e_R^- \rightarrow W^+W^-$ cross section on 500GeV(left) and 1TeV(right) ILC and caused by different anomalous coupling constants.

If we also suppose the same experimental relative uncertainty of cross section on polarized ILC as $\pm 5\%$, the polarized $\sqrt{s_{ee}} = 500$ GeV ILC can provide a better detection sensitivity on the anomalous coupling constants f_{27} :

$$-3.5 \times 10^{-2} \text{ TeV}^{-2} < f_{27}/\Lambda^2 < 3.5 \times 10^{-2} \text{ TeV}^{-2},$$

And for $\sqrt{s_{ee}} = 1$ TeV polarized ILC, the detection sensitivity is:

$$-9 \times 10^{-3} \text{ TeV}^{-2} < f_{27}/\Lambda^2 < 9 \times 10^{-3} \text{ TeV}^{-2},$$

Both anomalous coupling f_{27} and standard model couplings appear in same S channel Feynman diagrams, so the partial cross section is independent to the W outgoing angular and there is no kinematic difference between the anomalous coupling signal and standard model background. Although we can not find any effective cuts to improve the sensitivity of the right handed polarized electron-positron process, the detect ability of the polarized linear collider to detect anomalous coupling f_{27} is still improved by more than one order of magnitude compared to the unpolarized one.

CONCLUSIONS

In this paper, we study the different electron-positron colliders detect abilities on various effective Lagrangian coefficients of LEP2. We analysis the anomalous couplings' affects on the $e^+e^- \rightarrow W^+W^-$ cross sections at LEP2, polarized and unpolarized ILC with 500 and 1000 GeV collision energy. Our calculations show that the higher the collision energy, the greater the ability to detect anomalous couplings. The detect sensitivity can be improved by 3-4 orders of magnitude, only when the collision energy increases by several times. This work illustrates as example that the TeV energy linear colliders have great capability on precision measurement. The future linear colliders have multiple options, such as polarized electron-positron beam and high energy photon colliders. Such options are helpful to measure different vertices. The scheme with right handed polarized electrons is helpful on detect the Z boson anomalous couplings. In this paper, we only study the single parameter affect on the only process $e^+e^- \rightarrow W^+W^-$, any anomalous couplings beyond the detection limits can change the cross section obviously. If there are not deviations from standard model's cross section, then all the four anomalous couplings mentioned above are within the detection bounds. However, once the future measurement find the cross section deviation, it is difficult to figure out which anomalous coupling beyond the bound. In this case, the study on other processes is useful such as $e^+e^- \rightarrow ZZ(Z\gamma)$.

Acknowledgment: This work of B. Z. is supported by the National Science Foundation of China under Grant No. 11075086 and 11135003.

* Electronic address: zb@mail.tsinghua.edu.cn(Communication author)

- [1] W. Buchmuller and D. Wyler, Nucl. Phys. **B 268**, 621 (1986); C. J. C. Burgess and H. J. Schnitzer, Nucl. Phys. **B 228**, 464 (1983); C. N. Leung, S. T. Love, and S. Rao, Z. Phys. **C 31**, 433 (1986).
- [2] A. De Rujula, M. B. Gavela, P. Hernandez, and E. Masso, Nucl. Phys. **B 384**, 3 (1992); K. Hagiwara, S. Ishihara, R. Szalapski, and D. Zeppenfeld, Phys. Rev. **D 48**, 2182 (1993).
- [3] O. J. P. Eboli, M. C. Gonzalez-Garcia, S. M. Lietti, and S. F. Novaes, Phys. Lett. **B 478**, 199 (2000).
- [4] F. de Campos, M. C. Gonzalez-Garcia, S. M. Lietti, S. F. Novaes, and R. Rosenfeld, Phys. Lett. **B 435**, 407 (1998).
- [5] D. Zeppenfeld, hep-ph/0203123; T. Plehn, D. Rainwater, and D. Zeppenfeld, Phys. Rev. Lett. **88**, 051801 (2002).
- [6] H.-J. He, Y.-P. Kuang, C.-P. Yuan, and B. Zhang, Phys. Lett. **B 554**, 64 (2003).
- [7] B. Zhang, Y.-P. Kuang, H.-J. He, and C.-P. Yuan, Phys. Rev. **D 67**, 114024 (2003).
- [8] V. Barger, K. Cheung, A. Djouadi, B. A. Kniel, and P. M. Zerwas, Phys. Rev. **D 49**, 79 (1994); M. Kramer, J. Kuhn, M. L. Stong, and P. M. Zerwas, Z. Phys. **C 64**, 21 (1994); K. Hagiwara and M. Stong, Z. Phys. **C 62**, 99 (1994); J. F. Gunion, T. Han, and R. Sobey, Phys. Lett. **B 429**, 79 (1998); K. Hagiwara, S. Ishihara, J. Kamoshita, and B. A. Kniehl, Eur. Phys. J. **C 14**, 457 (2000).
- [9] V. Barger, T. Han, P. Langacker, B. McElrath, and P. M. Zerwas, Phys. Rev. **D 67**, 115001 (2003).
- [10] For a review on collider phenomenology, M.C. Gonzalez- Garcia, Int. J. Mod. Phys. **A 14**, 3121 (1999).
- [11] V. Barger, D. Marfatia, and K. Whisnant, Int. J. Mod. Phys. **E12**, 569 (2003); B. Kayser, p. 145 of the Review of Particle Physics, Phys. Lett. **B592**, 1 (2004).
- [12] P. Minkowski, Phys. Lett. **B67**, 421 (1977); R. N. Mohapatra and G. Senjanovic, Phys. Rev. Lett. **44**, 912 (1980). M. C. Gonzalez-Garcia and M. Maltoni, Phys. Rept. **460** (2008)1 ; R. N. Mohapatra and A. Y. Smirnov, Ann. Rev. Nucl. Part. Sci. **56** (2006) 569.
- [13] N. Arkani-Hamed, A. G. Cohen, H. Georgi, Phys. Lett. **B513**, 232-240 (2001); and, for a

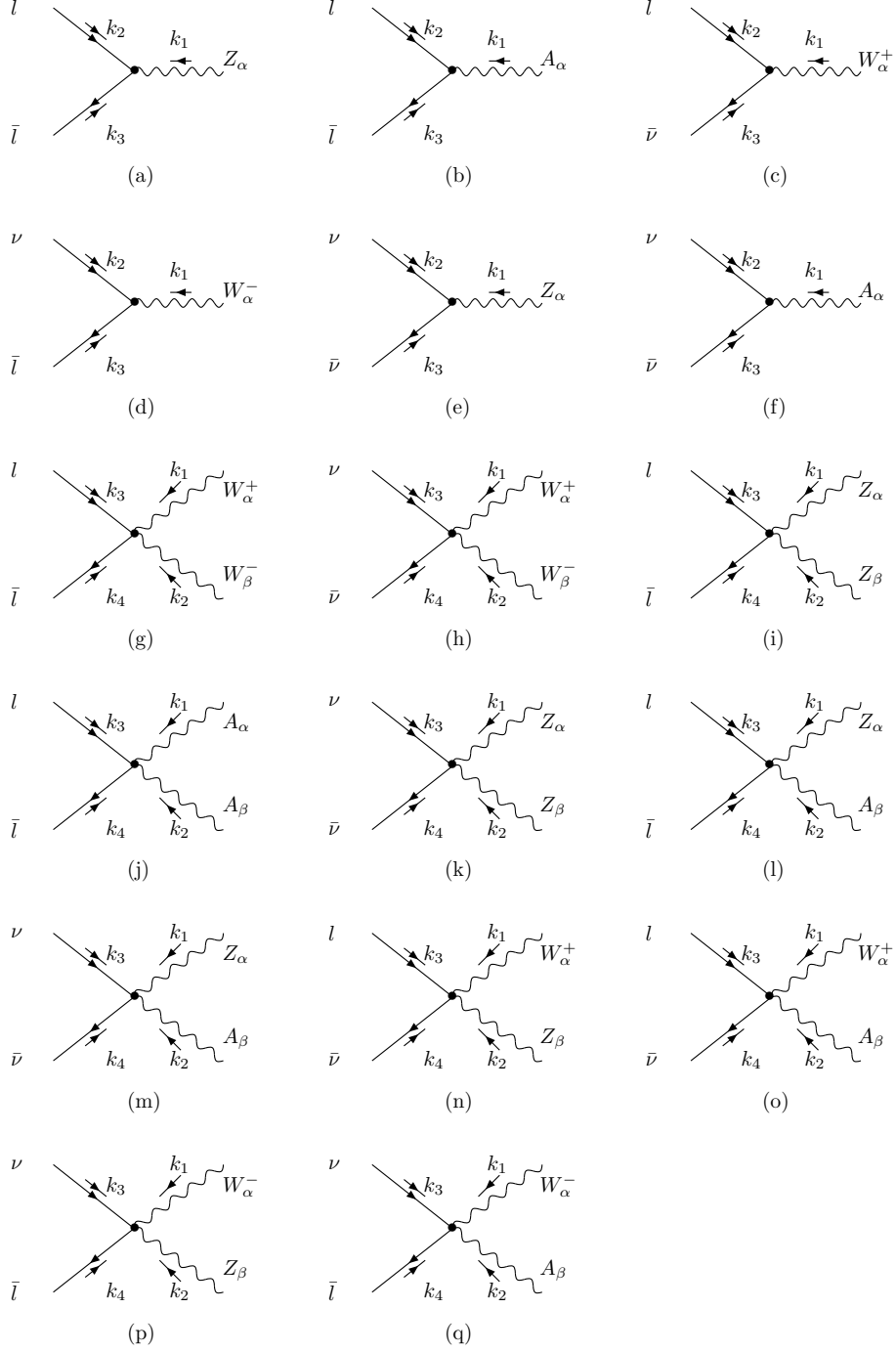
review, see M. Perelstein, Prog. Part. Nucl. Phys. **58**, 247 (2007).

- [14] C. Csaki, C. Grojean, H. Murayama, L. Pilo, and J. Terning, Phys. Rev. **D 69**, 055006 (2004);
C. Csaki, C. Grojean, L. Pilo, and J. Terning, Phys. Rev. Lett. **92**, 101802 (2004).
- [15] J. C. Pati and A. Salam, Phys. Rev. **D10**, 275 (1974); R. N. Mohapatra and J. C. Pati, Phys. Rev. **D11**, 566, 2558 (1975); G. Senjanovic and R. N. Mohapatra, Phys. Rev. **D12**, 1502 (1975).
- [16] L3 Collaboration, Phys.Lett.B600:22-40,2004
- [17] Particle Data Group, J.Phys. G: Nucl. Part. Phys. **33** (2006)1

APPENDIX

The Feynman rules of the dimension-6 leptonic anomalous gauge couplings:

$$\begin{aligned}
 (a) \quad & -\frac{1}{\Lambda^2} [k_1(k_2 - k_3)^\alpha - \gamma^\alpha k_1 \cdot (k_2 - k_3)] (\frac{c}{2} f_7 P_L + s f_{11} P_L + s f_{13} P_R) \\
 & + \frac{i}{\Lambda^2} [k_1 k_1^\alpha - k_1^2 \gamma^\alpha] (\frac{c}{2} f_{24} P_L + s f_{26} P_L + s f_{27} P_R) \\
 (b) \quad & -\frac{1}{\Lambda^2} [k_1(k_2 - k_3)^\alpha - \gamma^\alpha k_1 \cdot (k_2 - k_3)] (\frac{s}{2} f_7 P_L - c f_{11} P_L - c f_{13} P_R) \\
 & + \frac{i}{\Lambda^2} [k_1 k_1^\alpha - k_1^2 \gamma^\alpha] (\frac{s}{2} f_{24} P_L - c f_{26} P_L - c f_{27} P_R) \\
 (c) \quad & \frac{1}{\Lambda^2} [k_1(k_2 - k_3)^\alpha - \gamma^\alpha k_1 \cdot (k_2 - k_3)] (\frac{\sqrt{2}}{2} f_7 P_L) \\
 & + \frac{i}{\Lambda^2} [k_1 k_1^\alpha - k_1^2 \gamma^\alpha] (-\frac{\sqrt{2}}{2} f_{24} P_L) \\
 (d) \quad & \frac{1}{\Lambda^2} [k_1(k_2 - k_3)^\alpha - \gamma^\alpha k_1 \cdot (k_2 - k_3)] (\frac{\sqrt{2}}{2} f_7 P_L) \\
 & + \frac{i}{\Lambda^2} [k_1 k_1^\alpha - k_1^2 \gamma^\alpha] (-\frac{\sqrt{2}}{2} f_{24} P_L) \\
 (e) \quad & -\frac{1}{\Lambda^2} [k_1(k_2 - k_3)^\alpha - \gamma^\alpha k_1 \cdot (k_2 - k_3)] (-\frac{c}{2} f_7 P_L + s f_{11} P_L) \\
 & + \frac{i}{\Lambda^2} [k_1 k_1^\alpha - k_1^2 \gamma^\alpha] (-\frac{c}{2} f_{24} P_L + s f_{26} P_L)
 \end{aligned}$$



$$\begin{aligned}
 (f) \quad & -\frac{1}{\Lambda^2} [k_1(k_2 - k_3)^\alpha - \gamma^\alpha k_1 \cdot (k_2 - k_3)] \left(-\frac{s}{2} f_7 P_L - c f_{11} P_L\right) \\
 & + \frac{i}{\Lambda^2} [k_1 k_1^\alpha - k_1^2 \gamma^\alpha] \left(-\frac{s}{2} f_{24} P_L - c f_{26} P_L\right)
 \end{aligned}$$

$$(g) \quad \frac{g}{2\Lambda^2} [g^{\alpha\beta} (\not{k}_1 + \not{k}_2) + \gamma^\alpha (k_4 - k_1 - k_3)^\beta + \gamma^\beta (k_3 - k_2 - k_4)^\alpha] (f_7 P_L)$$

$$\begin{aligned}
& -\frac{ig}{2\Lambda^2}[g^{\alpha\beta}(\not{k}_1 - \not{k}_2) + \gamma^\alpha(k_4 - k_1 + k_3)^\beta + \gamma^\beta(-k_4 + k_2 - k_3)^\alpha](f_{24}P_L) \\
(h) \quad & \frac{g}{2\Lambda^2}[g^{\alpha\beta}(\not{k}_1 + \not{k}_2) + \gamma^\alpha(k_3 - k_1 - k_4)^\beta + \gamma^\beta(k_4 - k_2 - k_3)^\alpha](f_7P_L) \\
& + \frac{ig}{2\Lambda^2}[g^{\alpha\beta}(\not{k}_1 - \not{k}_2) + \gamma^\alpha(k_4 - k_1 + k_3)^\beta + \gamma^\beta(-k_4 + k_2 - k_3)^\alpha](f_{24}P_L) \\
(i) \quad & -\frac{g}{\Lambda^2}[g^{\alpha\beta}(\not{k}_1 + \not{k}_2) - \gamma^\alpha k_1^\beta - \gamma^\beta k_2^\alpha](\frac{2s^2 - 1}{2}f_7P_L + \frac{s(2s^2 - 1)}{c}f_{11}P_L + \frac{2s^3}{c}f_{13}P_R) \\
(j) \quad & \frac{g}{\Lambda^2}[g^{\alpha\beta}(\not{k}_1 + \not{k}_2) - \gamma^\alpha k_1^\beta - \gamma^\beta k_2^\alpha](s^2f_7P_L - 2csf_{11}P_L - 2csf_{13}P_R) \\
(k) \quad & \frac{g}{\Lambda^2}[g^{\alpha\beta}(\not{k}_1 + \not{k}_2) - \gamma^\alpha k_1^\beta - \gamma^\beta k_2^\alpha](\frac{1}{2}f_7P_L - \frac{s}{c}f_{11}P_L) \\
(l) \quad & \frac{g}{\Lambda^2}[g^{\alpha\beta}\not{k}_1 - \gamma^\alpha k_1^\beta](csf_7P_L + 2s^2f_{11}P_L) \\
& + \frac{g}{\Lambda^2}[g^{\alpha\beta}\not{k}_2 - \gamma^\beta k_2^\alpha](-\frac{s(2s^2 - 1)}{2c}f_7P_L + (2s^2 - 1)f_{11}P_L) \\
(m) \quad & \frac{g}{\Lambda^2}[g^{\alpha\beta}\not{k}_2 - \gamma^\beta k_2^\alpha](\frac{s}{2c}f_7P_L + f_{11}P_L) \\
(n) \quad & -\frac{g}{\Lambda^2}\frac{\sqrt{2}}{2}c[\gamma^\alpha(k_3 - k_4)^\beta - \gamma^\beta(k_3 - k_4)^\alpha]f_7P_L \\
& + \frac{g}{\Lambda^2}\frac{\sqrt{2}s^2}{2c}[g^{\alpha\beta}\not{k}_1 - \gamma^\alpha k_1^\beta]f_7P_L \\
& - \frac{g}{\Lambda^2}\sqrt{2}s[g^{\alpha\beta}\not{k}_2 - \gamma^\beta k_2^\alpha]f_{11}P_L \\
& - \frac{ig}{\Lambda^2}\frac{\sqrt{2}c}{2}[g^{\alpha\beta}(\not{k}_1 - \not{k}_2) - \gamma^\alpha(2k_1 + k_2)^\beta + \gamma^\beta(k_1 + 2k_2)^\alpha]f_{24}P_L \\
(o) \quad & -\frac{g}{\Lambda^2}\frac{\sqrt{2}}{2}s[\gamma^\alpha(k_3 - k_4)^\beta - \gamma^\beta(k_3 - k_4)^\alpha]f_7P_L \\
& - \frac{g}{\Lambda^2}\frac{\sqrt{2}s}{2}[g^{\alpha\beta}\not{k}_1 - \gamma^\alpha k_1^\beta]f_7P_L \\
& + \frac{g}{\Lambda^2}\sqrt{2}c[g^{\alpha\beta}\not{k}_2 - \gamma^\beta k_2^\alpha]f_{11}P_L \\
& - \frac{ig}{\Lambda^2}\frac{\sqrt{2}s}{2}[g^{\alpha\beta}(\not{k}_1 - \not{k}_2) - \gamma^\alpha(2k_1 + k_2)^\beta + \gamma^\beta(k_1 + 2k_2)^\alpha]f_{24}P_L
\end{aligned}$$

$$\begin{aligned}
(p) \quad & \frac{g}{\Lambda^2} \frac{\sqrt{2}}{2} c [\gamma^\alpha (k_3 - k_4)^\beta - \gamma^\beta (k_3 - k_4)^\alpha] f_7 P_L \\
& + \frac{g}{\Lambda^2} \frac{\sqrt{2} s^2}{2c} [g^{\alpha\beta} \not{k}_1 - \gamma^\alpha k_1^\beta] f_7 P_L \\
& - \frac{g}{\Lambda^2} \sqrt{2} s [g^{\alpha\beta} \not{k}_2 - \gamma^\beta k_2^\alpha] f_{11} P_L \\
& + \frac{ig}{\Lambda^2} \frac{\sqrt{2} c}{2} [g^{\alpha\beta} (\not{k}_1 - \not{k}_2) - \gamma^\alpha (2k_1 + k_2)^\beta + \gamma^\beta (k_1 + 2k_2)^\alpha] f_{24} P_L \\
\\
(q) \quad & \frac{g}{\Lambda^2} \frac{\sqrt{2}}{2} s [\gamma^\alpha (k_3 - k_4)^\beta - \gamma^\beta (k_3 - k_4)^\alpha] f_7 P_L \\
& - \frac{g}{\Lambda^2} \frac{\sqrt{2} s}{2} [g^{\alpha\beta} \not{k}_1 - \gamma^\alpha k_1^\beta] f_7 P_L \\
& + \frac{g}{\Lambda^2} \sqrt{2} c [g^{\alpha\beta} \not{k}_2 - \gamma^\beta k_2^\alpha] f_{11} P_L \\
& + \frac{ig}{\Lambda^2} \frac{\sqrt{2} s}{2} [g^{\alpha\beta} (\not{k}_1 - \not{k}_2) - \gamma^\alpha (2k_1 + k_2)^\beta + \gamma^\beta (k_1 + 2k_2)^\alpha] f_{24} P_L
\end{aligned}$$